DOI: 10.13009/EUCASS2019-94

Differential Game Guidance Law on Evader in Bearing-only Information Applications

Guo Hao, Yu Zhuoyang, Wang Xun and Chen Xuan
Science and Technology on Space Physics Laboratory
Beijing, 100076, China

Abstract

For improving the evasion performance of evader, a novel real time maneuver differential game guidance law with the time delay of battlefield situation awareness from bearing-only information is proposed. Based on the azimuth and elevation rates of the line of sight, a three-dimensional dynamic model about the pursuit-evasion is established. For getting situation information containing the pursuit games about pursuer and the pursuit-evasion relative states via bearings-only information, a pseudo-measurement gain Kalman filter is designed. A new differential game guidance law with correcting first order response dynamics of evader and the time delay of the pseudo-measurement gain Kalman filter information is proposed. Finally, the superior maneuver evasion performance and practicability in engineering besides adequately utilizing the battlefield situation awareness of the new differential game guidance law is verified by computer simulations.

1. Introduction

To enhance the evasive performance of all kinds of aircrafts is highly important with the development of the antimissile and aerial defense. The modern interceptors are of high maneuverability and over loading, so that aircraft as an evader has to aware the battlefield situation information and has a superior evasive guidance law. Otherwise, the one-sided optimization game is only considered to give the evasive guidance law. However, the problem in this paper, interceptor and aircraft with the battlefield situation awareness, is best modeled to use two players, that is, it becomes a two-sided optimization problem. The aircrafts interception game is a zero-sum two-player game, furthermore of a type referred to as a pursuit-evasion game. This dynamic problem can be described by zero-sum pursuit-evasion differential game theory [1], [2]. As a real time maneuver game, the differential game guidance law (DGL) can adequately consider the relative state information about pursuer and evader, which is deserved to research on evasive game.

Optimal guidance law (OGL) on evasive maneuver strategy has traditionally been developed with one-sided optimization game. Optimal control theory is usually applied, assuming perfect information [3]. Knowing the pursuit strategy of the incoming pursuer, the evader can acquire the optimal maneuver evasive guidance law. Shinar and Steinberg [4] analyzed the optimal evasion strategy with two-dimensional linear kinematics, first-order dynamics and limited value of pursuer and evader acceleration, where the pursuer is foregone to the classical proportional navigation (PN) guidance law. The optimal evasive maneuver guidance law was almost always of the bang-bang structure, which derived from the closed-form solution for first-order dynamic models and effective navigation ratio. Ben-Asher et al. [5] also obtained the bang-bang type evasion guidance law for evader with a path-angle constraint and against more than one pursuer. Forte et al. [6] investigated the same model as the Ref. [4], but with nonlinear kinematics. The optimal evasive maneuver guidance law was almost also of the bang-bang type. These one-sided optimal evasive maneuver strategies via optimal control theory need to know the pursuit guidance laws of the incoming pursuer, which is usually impossibility in actual engagement. Nevertheless, DGL considering two-sided optimization in this paper does not need to know the pursuit strategy, being excellent to the one-sided OGL.

Differential game theory is more used to interception of highly maneuvering targets [2], [7]-[10]. Shima et al. [7] and Chen et al. [8] transformed pursuit-evasion problem into a linear differential game. The engagement between two objects with first-order dynamics, constant bounds on the lateral accelerations, and time varying with compensation of the estimation delay was investigated by Shima et al. [7]. Considering about a prespecified impact angle, a nonlinear zero-sum differential game framework is posed by Bardhan and Ghose [9]. The impact-angle-constrained guidance law is projected terminal impact angle error and effective to two-dimensional engagement. Pontani and Conway [2] presented a direct numerical method to find the saddle-point trajectories for a zero-sum pursuit-evasion differential game about the interception of ballistic missile warheads. Then the effect and robustness of their method

DOI: 10.13009/EUCASS2019-94

for solution of that game is validated. The solution of saddle-point trajectories for differential game is valuable to analysis all the pursuit and evasion, but only interception strategy is their attention all the same in Ref. [2]. In addition, the DGL above is analyzed on the premise that two players in engagement can obtain the entire battlefield situation. In Ref. [10], the pursuit DGL is generated by the different estimation error of evader's acceleration. But the estimation error is directly calculated by the estimated and actual acceleration of evader, which is obvious impossibility in actual pursuit-evasion engagement, and the performance of DGL directly using the actual acceleration is obviously better than that in Ref. [10].

In recent work [11], [12], a three-player cooperative differential game was investigated in solving the target-missile-defender interception problem. The target and defender shared noisy measurements on the interception missile, and attacker obtained his optimal strategy to minimize the miss distance between itself and the missile. However, zero-sum differential game with battlefield situation awareness information on one-on-one evasion guidance law in two-sided optimization problem application is few in the present literature. A novel real time maneuver evasive DGL with the time delay of battlefield situation awareness from bearing-only information is proposed in this work.

The paper is organized as follows. Section 2 builds three dimensional engagement dynamic models based on light of sight (LOS). Next, in Section 3, a pseudo-measurement gain Kalman filter (PMGKF) is devised by pseudo-linear measurement formula using trigonometric function. All the information needed about the relative distance, approach velocity and pursuer's acceleration can be obtained via this filter, and the first order response dynamics is becoming to describe the filter result. Then, in Section 4, the optimal evasive strategy is derived from game solution with the time dalay from PMGKF. The numerical simulation is given in Section 5, and Section 6 comcludes the paper with a summary of the main results.

2. Engagement Formulation Based on LOS

For using the information about LOS to build the three dimensional dynamic model of the pursuit-evasion, three coordinate system is defined in this paper.

(1) Inertial coordinate system O-XYZ: the origin O is collocated with the initial evader position. The X-axis is aligned with the initial LOS direction and the Y-axis is constrained in the direction of the evader velocity vector. The Z-axis is defined by right-handed Cartesian coordinate.

(2) Translational coordinate system O_T-$X_TY_TZ_T$: the origin O_T is collocated with the evader position all the time. Each axis is always parallel to the corresponding axis of inertial coordinate system.

(3) LOS coordinate system O_L-$X_LY_LZ_L$: the origin O_L is the same as O_T. The X_L-axis is aligned with the LOS direction and the Z_L-axis is orthogonal to the X_L-axis in the $X_TO_TZ_T$ plane. The X_L, Y_L and Z_L-axis compose right-handed Cartesian coordinate.

Figure 1 shows the transformation from translational coordinate system to LOS coordinate system; ψ_L is the LOS azimuth angle, φ_L is the LOS elevation angle. Its coordinate transformation can be described as follows:

$$\begin{bmatrix} x_L^0 \\ y_L^0 \\ z_L^0 \end{bmatrix} = \boldsymbol{L_T} \begin{bmatrix} x_T^0 \\ y_T^0 \\ z_T^0 \end{bmatrix} \tag{1}$$

where,

$$\boldsymbol{L_T} = M_3[\varphi_L]M_2[\psi_L] = \begin{bmatrix} \cos\varphi_L\cos\psi_L & \sin\varphi_L & -\cos\varphi_L\sin\psi_L \\ -\sin\varphi_L\cos\psi_L & \cos\varphi_L & \sin\varphi_L\sin\psi_L \\ \sin\psi_L & 0 & \cos\psi_L \end{bmatrix} \tag{2}$$

Note the pursuer position in translational coordinate system as $\boldsymbol{x} = (x, y, z)^T$, so the pursuer velocity and acceleration relative to evasion in inertial coordinate can be express as:

Relative velocity $\boldsymbol{v} = \left(\dot{x}, \dot{y}, \dot{z}\right)^T$;

Relative acceleration $\boldsymbol{a} = \left(\ddot{x}, \ddot{y}, \ddot{z}\right)^T$.

Note that R and $\dot{R}$ are the pursuer and evader relative range and approach velocity; R_{13} and $\dot{R}_{13}$ are the projections of R and $\dot{R}$ in the $X_TO_TZ_T$ plane; the engagement geometry can be expressed as the differential formula follows.

$$\begin{bmatrix} \dot{R} \\ 0 \\ 0 \end{bmatrix} + \boldsymbol{\omega} \times \begin{bmatrix} R \\ 0 \\ 0 \end{bmatrix} = \boldsymbol{L_T} \begin{bmatrix} \dot{x} \\ \dot{y} \\ \dot{z} \end{bmatrix} = \begin{bmatrix} \dot{x}\cos\varphi_L\cos\psi_L + \dot{y}\sin\varphi_L - \dot{z}\cos\varphi_L\sin\psi_L \\ -\dot{x}\sin\varphi_L\cos\psi_L + \dot{y}\cos\varphi_L + \dot{z}\sin\varphi_L\sin\psi_L \\ \dot{x}\sin\psi_L + \dot{z}\cos\psi_L \end{bmatrix} \tag{3}$$

$$\dot{R}_{13} = \dot{x}\cos\psi_L - \dot{z}\sin\psi_L \tag{4}$$

DOI: 10.13009/EUCASS2019-94

where $\boldsymbol{\omega} = \left[\dot{\psi}_L \sin\varphi_L \quad \dot{\psi}_L \cos\varphi_L \quad \dot{\varphi}_L\right]^T$ denotes the vector of LOS-translational coordinate system relative angle rate. After differential and linearization on Eq. (3) and Eq. (4), the corresponding equation becomes

$$\begin{cases} \ddot{\varphi}_L = -\dfrac{2\dot{R}}{R}\dot{\varphi}_L + \dfrac{1}{R}(-\ddot{x}\sin\varphi_L\cos\psi_L + \ddot{y}\cos\varphi_L + \ddot{z}\sin\varphi_L\sin\psi_L) \\ \ddot{\psi}_L = -\dfrac{2\dot{R}_{13}}{R_{13}}\dot{\psi}_L - \dfrac{1}{R_{13}}\left(\ddot{x}\sin\psi_L + \ddot{z}\cos\psi_L\right) \end{cases} \tag{5}$$

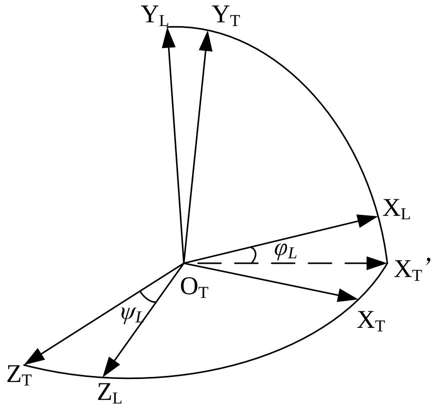

Figure 1 Coordinate transformation from translational coordinate system to LOS coordinate system

Note that the actual accelerations of pursuer and evader in LOS coordinate system are $\boldsymbol{a}_{\mathrm{P}} = [v_x, v_y, v_z]^T$ and $\boldsymbol{a}_{\mathrm{E}} = [u_x, u_y, u_z]^T$, respectively, hence,

$$\begin{bmatrix} v_x \\ v_y \\ v_z \end{bmatrix} - \begin{bmatrix} u_x \\ u_y \\ u_z \end{bmatrix} = \boldsymbol{L_T}\begin{bmatrix} \ddot{x} \\ \ddot{y} \\ \ddot{z} \end{bmatrix} = \begin{bmatrix} \ddot{x}\cos\varphi_L\cos\psi_L + \ddot{y}\sin\varphi_L - \ddot{z}\cos\varphi_L\sin\psi_L \\ -\ddot{x}\sin\varphi_L\cos\psi_L + \ddot{y}\cos\varphi_L + \ddot{z}\sin\varphi_L\sin\psi_L \\ \ddot{x}\sin\psi_L + \ddot{z}\cos\psi_L \end{bmatrix} \tag{6}$$

Substituting Eq. (6) into Eq. (5) yields the expression

$$\begin{cases} \ddot{\varphi}_L = -\dfrac{2\dot{R}}{R}\dot{\varphi}_L - \dfrac{1}{R}u_y + \dfrac{1}{R}v_y \\ \ddot{\psi}_L = -\dfrac{2\dot{R}_{13}}{R_{13}}\dot{\psi}_L + \dfrac{1}{R_{13}}u_z - \dfrac{1}{R_{13}}v_z \end{cases} \tag{7}$$

Consider the evader with first order response dynamics:

$$\dot{\boldsymbol{a}}_{\mathrm{E}} = \frac{\boldsymbol{u}^c - \boldsymbol{a}_{\mathrm{E}}}{\tau_{\mathrm{E}}} \tag{8}$$

where τ_{E} is the evader's time constant, $\boldsymbol{u}^c = [u_y^c, u_z^c]^T$ denotes the vector of the evader's command acceleration. From Eq. (7), relative distance, approach velocity and pursuer's acceleration are requirement.

3. Gaining Information Needed via Pseudo- measurement Gain Kalman Filter

The bearing-only information can be mathematically described by a linear state equation and a nonlinear measurement model, which is a nonlinearities filter problem in fact. Non-recursive representations of the traditional extended Kalman Filter are often more tractable, despite their computational inefficiency [13]. To improve algorithm stability, a pseudo-measurement gain Kalman filter (PMGKF) is built in this section by pseudo-linear measurement formula using trigonometric function.

3.1 Building PMGKF

The pursuer's acceleration in translational coordinate system can be described by Singer model:

$$\dot{\boldsymbol{a}}_{\mathrm{PT}} = -\alpha\boldsymbol{a}_{\mathrm{PT}} + \boldsymbol{\omega} \tag{9}$$

DOI: 10.13009/EUCASS2019-94

where $\boldsymbol{a}_{PT} = [a_{Px}, a_{Py}, a_{Pz}]^T$ denotes pursuer's acceleration in translational coordinate system, α is pursuer's maneuver frequency, reciprocal of its time constant; $\boldsymbol{\omega}$ is the zero-mean white noise sequence with variance $2\alpha\sigma^2$, σ^2 is variance of pursuer's acceleration.

Hence linear system state model is given as follows:

$$\dot{\boldsymbol{X}} = \boldsymbol{F}\boldsymbol{X} + \boldsymbol{G}\boldsymbol{a}_{ET} + \boldsymbol{K}\boldsymbol{\omega} \tag{10}$$

where $\boldsymbol{X} = [x, y, z, \dot{x}, \dot{y}, \dot{z}, a_{Px}, a_{Py}, a_{Pz}]^T$ denotes the state vector, $\boldsymbol{F} = \begin{bmatrix} \boldsymbol{O}_3 & \boldsymbol{I}_3 & \boldsymbol{O}_3 \\ \boldsymbol{O}_3 & \boldsymbol{O}_3 & \boldsymbol{I}_3 \\ \boldsymbol{O}_3 & \boldsymbol{O}_3 & -\alpha\boldsymbol{I}_3 \end{bmatrix}$, $\boldsymbol{G} = \begin{bmatrix} \boldsymbol{O}_3 \\ -\boldsymbol{I}_3 \\ \boldsymbol{O}_3 \end{bmatrix}$, $\boldsymbol{K} = \begin{bmatrix} \boldsymbol{O}_3 \\ \boldsymbol{O}_3 \\ \boldsymbol{I}_3 \end{bmatrix}$. $\boldsymbol{O}_3$ is a matrix with three rows and three columns with all elements equal to zero, and $\boldsymbol{I}_3$ is an identity matrix with three dimensions, $\boldsymbol{a}_{ET}$ is the evader's acceleration in translational coordinate system.

Accordingly the discrete-time state estimation is

$$\boldsymbol{X}(k+1) = \boldsymbol{\Phi}(k)\boldsymbol{X}(k) + \boldsymbol{G}(k)\boldsymbol{a}_{ET}(k) + \boldsymbol{Q}(k) \tag{11}$$

$$\begin{cases} \boldsymbol{\Phi}(k) = e^{\boldsymbol{F}\cdot T_S} \\ \boldsymbol{G}(k) = \int_0^{T_S} \boldsymbol{\Phi}(\tau)\boldsymbol{G}d\tau \\ \boldsymbol{Q}(k) = \int_0^{T_S} \boldsymbol{\Phi}(\tau)\boldsymbol{Q}_k\boldsymbol{\Phi}^T(\tau)d\tau \\ \boldsymbol{Q}_k = E((\boldsymbol{K}\boldsymbol{\omega})\cdot(\boldsymbol{K}\boldsymbol{\omega})^T) \end{cases} \tag{12}$$

T_S is sampling interval.

For gaining PMGKF with bearing-only information, pseudo-measurement gain Kalman observation (PMGKO) is built firstly. The nonlinear measurement equation with bearing-only information is

$$\begin{bmatrix} \varphi_L \\ \psi_L \end{bmatrix} = h(\boldsymbol{X}) + \boldsymbol{\eta} = \begin{bmatrix} \arctan\dfrac{y}{\sqrt{x^2+z^2}} \\ \arctan\dfrac{-z}{x} \end{bmatrix} + \begin{bmatrix} \eta_1 \\ \eta_2 \end{bmatrix} \tag{13}$$

where $\boldsymbol{\eta}$ is observation noise. Single observation error is little with precision observation; hence Eq. (13) can be described as pseudo-linear form below:

$$\boldsymbol{0}_2 = \boldsymbol{H}(k)\boldsymbol{X}(k) + \boldsymbol{\upsilon}(k) \tag{14}$$

where $\boldsymbol{0}_2$ is two-dimensional zero vector, $\boldsymbol{\upsilon} = [R\eta_1, R_{13}\eta_2]^T$, $\boldsymbol{H} = \left[\begin{bmatrix} \cos\psi_L \sin\varphi_L & -\cos\varphi_L & -\sin\psi_L\sin\varphi_L \\ \sin\psi_L & 0 & \cos\psi_L \end{bmatrix}, \boldsymbol{O}_{2\times 6}\right]$, $\boldsymbol{O}_{2\times 6}$ is a matrix with two rows and six columns with all elements equal to zero. In PMGKO, pseudo-measurement matrix $\boldsymbol{V}(k)$ is

$$\boldsymbol{V}(k) = E(\boldsymbol{\upsilon}\boldsymbol{\upsilon}^T) = \boldsymbol{D}(k)E(\boldsymbol{\eta}\boldsymbol{\eta}^T)\boldsymbol{D}^T(k) \tag{15}$$

where relative distance matrix $\boldsymbol{D}(k)$ is

$$\boldsymbol{D}(k) = \begin{bmatrix} R(k) & 0 \\ 0 & R_{13}(k) \end{bmatrix} \tag{16}$$

From Eq. (15) and Eq. (16), pseudo-measurement noise variance is time varying in PMGKO, but the actual relative distance between purser and evader cannot be gained, while the one-step-ahead prediction value is used to calculate its approximation:

$$\tilde{\boldsymbol{D}}(k) = \begin{bmatrix} R(k\,|\,k-1) & 0 \\ 0 & R_{13}(k\,|\,k-1) \end{bmatrix} \tag{17}$$

As stated previously, PMGKF can be accomplished with the following steps.

1) The one-step-ahead prediction of state and error matrix is

$$\hat{\boldsymbol{X}}(k\,|\,k-1) = \boldsymbol{\Phi}(k\,|\,k-1)\hat{\boldsymbol{X}}(k-1\,|\,k-1) + \boldsymbol{G}(k\,|\,k-1)\hat{\boldsymbol{a}}_m(k-1\,|\,k-1) \tag{18}$$

$$\boldsymbol{M}(k\,|\,k-1) = \boldsymbol{\Phi}(k\,|\,k-1)\boldsymbol{M}(k-1\,|\,k-1)\boldsymbol{\Phi}^T(k\,|\,k-1) + \boldsymbol{Q}(k) \tag{19}$$

2) The pseudo-measurement noise variance is

$$\boldsymbol{V}(k) = \tilde{\boldsymbol{D}}(k)E(\boldsymbol{\eta}\boldsymbol{\eta}^T)\tilde{\boldsymbol{D}}^T(k) \tag{20}$$

3) The filter plus matrix is

$$\boldsymbol{K}(k) = \boldsymbol{M}(k\,|\,k-1)\boldsymbol{H}^T(k)\left[\boldsymbol{H}^T(k)\boldsymbol{M}(k\,|\,k-1)\boldsymbol{H}(k) + \boldsymbol{V}(k)\right]^{-1} \tag{21}$$

4) The update of state and error matrix is

DOI: 10.13009/EUCASS2019-94

$$\hat{\boldsymbol{X}}(k \mid k) = \hat{\boldsymbol{X}}(k \mid k-1) + \boldsymbol{K}(k)\left(-\boldsymbol{H}(k)\hat{\boldsymbol{X}}(k \mid k-1)\right) \tag{22}$$

$$\boldsymbol{M}(k \mid k) = \left[\boldsymbol{I}_9 - \boldsymbol{K}(k)\boldsymbol{H}(k)\right]\boldsymbol{M}(k \mid k-1) \tag{23}$$

3.2 Numerical estimation result

In this simulation, sampling interval is 0.01s, observation variance $E(\boldsymbol{\eta}\boldsymbol{\eta}^T)$ = 0.001rad^2. Hypothetically purser can get the needed information about evader, using proportional navigation with effective navigation ratio N' = 4. Evader captures purser in 60km relative distance, and begins maneuvering with sine law as follows:

$$\begin{cases} u_y^c = 7g\sin(0.5t) \\ u_z^c = -7g\sin(0.5t) \end{cases} \tag{24}$$

where g = 9.8 m·s^{-2} denotes the acceleration of gravity, t is time.
Initial parameter of the simulation is shown in Table 1, the vectors of location and velocity is the value in inertial coordinate system.

Table 1 Initial parameter of the simulation

	Pursuer	Evader
Position/m	(60000, 0, 0)	(0, 0, 0)
Volicity/(m·s^{-1})	(-1616.8, 674.22, -413.81)	(3347.8, 1020.8, 0)
Acceleration/(m·s^{-2})	(0, 0, 0)	(0, 0, 0)
Time constant/s	0.5	1.5
Maximum acceleration/(m·s^{-2})	196	68.6

From Table 1, the actual initial state $\boldsymbol{X}$ = [60000, 0, 0, -4964.6, -346.58, -413.81, 0, 0, 0]^T while the filter initial state $\hat{\boldsymbol{X}}$ = [59000, -100, 100, -5000, -350, -410, 0, 0, 0]^T and the initial variance matrix $\boldsymbol{Q}$ = diag([10000, 10000, 10000, 100, 100, 100, 0.1, 0.1, 0.1]).
Figure 2 shows the estimation of the pursuer's elevation acceleration that is the projection in Y_L-axis using the PMGKF, and Figure 3 shows the result of azimuth acceleration that is the projection in Z_L-axis. Estimated error of acceleration is given in Figure 4.
Notice that the estimation delays when the pursuer's acceleration changes from Figure 2 and Figure 3. The inherent delay is used to estimate a maneuver from the time [7]. Here, the time delay is about 0.5s that is the same as the time constant of pursuer, so the estimated acceleration on pursuer can be described by the first order response dynamics:

$$\dot{\boldsymbol{v}}^p = \frac{\boldsymbol{a}_\mathrm{P} - \boldsymbol{v}^p}{\tau_\mathrm{P}} \tag{25}$$

where τ_P is the pursuer's time constant, $\boldsymbol{v}^p = [v_y^p, v_z^p]^T$, is the estimated acceleration on pursuer. Figure 5 shows the comparisons about calculate value using the pursuer actual acceleration based on Eq. (25) and the estimated result by PMGKF.
Notice that the first order response dynamics is becoming to describe the filter result.

4. Game Solution with the Time Delay from PMGKF

Based on Eq. (7), (8) and (25), a linear state model is built as follows:

$$\dot{\boldsymbol{x}} = \boldsymbol{A}\boldsymbol{x} + \boldsymbol{B}\boldsymbol{u}^c + \boldsymbol{C}\boldsymbol{a}_\mathrm{P} \tag{26}$$

where $\boldsymbol{x} = [\dot{\varphi}_L, u_y, v_y^p, \dot{\psi}_L, u_z, v_z^p]^T$, $\boldsymbol{A}$ = diag($\boldsymbol{A}_1$, $\boldsymbol{A}_2$),

$$\boldsymbol{A}_1 = \begin{bmatrix} -\frac{2\dot{R}}{R} & -\frac{1}{R} & 0 \\ 0 & -\frac{1}{\tau_\mathrm{E}} & 0 \\ 0 & 0 & -\frac{1}{\tau_\mathrm{P}} \end{bmatrix}, \quad \boldsymbol{A}_2 = \begin{bmatrix} -\frac{2\dot{R}_{13}}{R_{13}} & \frac{1}{R_{13}} & 0 \\ 0 & -\frac{1}{\tau_\mathrm{E}} & 0 \\ 0 & 0 & -\frac{1}{\tau_\mathrm{P}} \end{bmatrix}, \quad \boldsymbol{B} = \begin{bmatrix} 0, \frac{1}{\tau_\mathrm{E}}, 0, 0, 0, 0 \\ 0, 0, 0, 0, \frac{1}{\tau_\mathrm{E}}, 0 \end{bmatrix}^T, \quad \boldsymbol{C} = \begin{bmatrix} \frac{1}{R}, \frac{1}{\tau_\mathrm{P}}, 0, 0, 0, 0 \\ 0, 0, 0, 0, \frac{1}{R_{13}}, \frac{1}{\tau_\mathrm{P}} \end{bmatrix}^T.$$

A differential game is formulated for Eq. (26) with the performance index

DOI: 10.13009/EUCASS2019-94

$$J=\frac{1}{2}\left(\boldsymbol{D}\boldsymbol{x}\left(t_f\right)\right)^T\boldsymbol{Q}\left(\boldsymbol{D}\boldsymbol{x}\left(t_f\right)\right)+\frac{1}{2}\int_{t_0}^{t_f}\left(-\boldsymbol{u}^{cT}\boldsymbol{C}_1\boldsymbol{u}^c+\boldsymbol{a}^{pT}\boldsymbol{C}_2\boldsymbol{a}^p\right)dt \tag{27}$$

where $\boldsymbol{D}=\begin{bmatrix}1&0&0&0&0&0\\0&0&0&1&0&0\end{bmatrix}$; $\boldsymbol{Q}$, $\boldsymbol{C}_1$, $\boldsymbol{C}_2$ are all the 2×2 positive definite diagonal matrix; t_0 and t_f are the initial and final time of the game, respectively. The evader aims to maximize the performance index J by controlling $\boldsymbol{u^c}$, while the pursuer wishes to minimize it using strategy $\boldsymbol{a}_{\mathrm{P}}$. Both evader's and pursuer's strategies are bounded:

$$\begin{cases}\left|\boldsymbol{u}^c\right|\le\boldsymbol{u}_{\max}^c\\\left|\boldsymbol{a}_{\mathrm{p}}\right|\le\boldsymbol{a}_{\mathrm{p}\max}\end{cases} \tag{28}$$

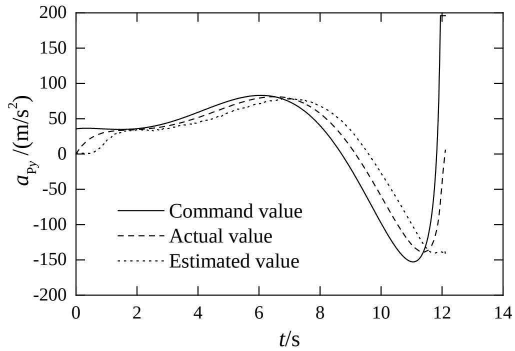

Figure 2 Comparison of elevation acceleration

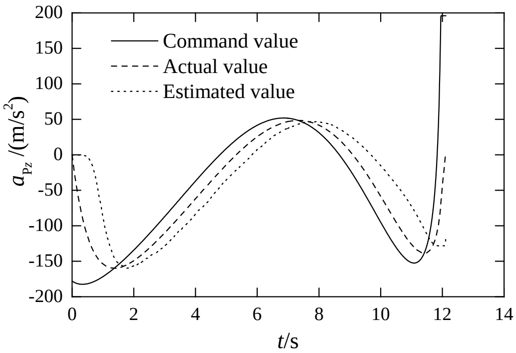

Figure 3 Comparison of azimuth acceleration

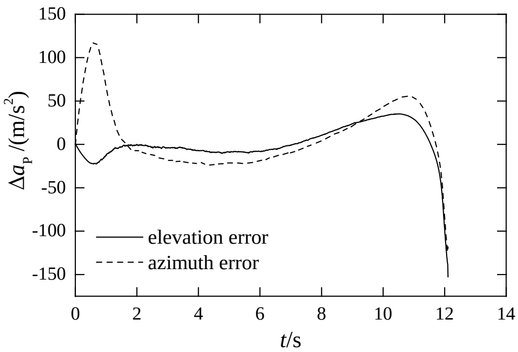

Figure 4 Estimated error of acceleration

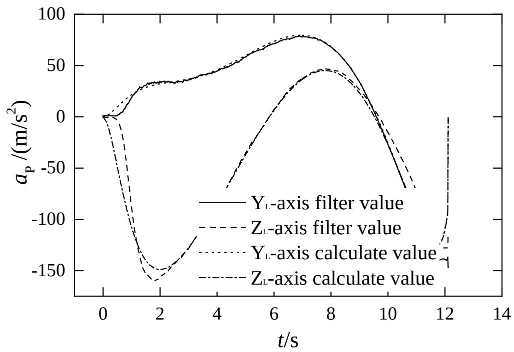

Figure 5 Comparisons about filter and calculate results

For sampling the system, a new state vector is defined:

$$\boldsymbol{Z}(t)=\boldsymbol{D}\boldsymbol{\Phi}(t_f,t)\boldsymbol{x}(t) \tag{29}$$

where $\boldsymbol{\Phi}(t_f, t)$ is the state translation matrix, it can be calculated from $\dot{\boldsymbol{x}}=\boldsymbol{A}\boldsymbol{x}$.

$$\boldsymbol{\Phi}\left(t_f,t\right)=e^{\boldsymbol{A}\left(t_f-t\right)}=e^{\boldsymbol{A}t_g} \tag{30}$$

where t_g is estimated by the formula:

$$t_g=-\frac{R}{\dot{R}} \tag{31}$$

Hence $\boldsymbol{Z}(t)$ is satisfied the differential equation:

$$\dot{\boldsymbol{Z}}=\boldsymbol{D}\boldsymbol{\Phi}\boldsymbol{B}\boldsymbol{u}^c+\boldsymbol{D}\boldsymbol{\Phi}\boldsymbol{C}\boldsymbol{v}^c \tag{32}$$

and the cost function changes into:

$$J=\frac{1}{2}\left(\boldsymbol{Z}\left(t_f\right)\right)^T\boldsymbol{Q}\left(\boldsymbol{Z}\left(t_f\right)\right)+\frac{1}{2}\int_{t_0}^{t_f}\left(-\boldsymbol{u}^{cT}\boldsymbol{C}_1\boldsymbol{u}^c+\boldsymbol{a}^{pT}\boldsymbol{C}_2\boldsymbol{a}^p\right)dt \tag{33}$$

Based on the Eq. (32) and (33), the Hamiltonian is

$$H=\frac{1}{2}\left(-\boldsymbol{u}^{cT}\boldsymbol{C}_1\boldsymbol{u}^c+\boldsymbol{a}^{pT}\boldsymbol{C}_2\boldsymbol{a}^p\right)+\boldsymbol{\lambda}^T\left(\boldsymbol{D}\boldsymbol{\Phi}\boldsymbol{B}\boldsymbol{u}^c+\boldsymbol{D}\boldsymbol{\Phi}\boldsymbol{C}\boldsymbol{a}^p\right) \tag{34}$$

where $\boldsymbol{\lambda}$ is the co-state variable, and it is satisfied the following co-state equation

DOI: 10.13009/EUCASS2019-94

$$\begin{cases} \dot{\boldsymbol{\lambda}} = -\dfrac{\partial H}{\partial \boldsymbol{Z}} = 0 \\ \lambda\left(t_f\right) = -\boldsymbol{QZ}\left(t_f\right) \end{cases} \tag{35}$$

The solution of co-state variable Eq. (35) is

$$\lambda\left(t\right) = -\boldsymbol{QZ}\left(t_f\right) \tag{36}$$

By the optimal conditions

$$\begin{cases} \dfrac{\partial H}{\partial \boldsymbol{u}^c} = -\boldsymbol{C}_1\boldsymbol{u}^c + \boldsymbol{B}^T\boldsymbol{\Phi}^T\boldsymbol{D}^T\boldsymbol{\lambda} = 0 \\ \dfrac{\partial H}{\partial \boldsymbol{a}^p} = \boldsymbol{C}_2\boldsymbol{a}^p + \boldsymbol{C}^T\boldsymbol{\Phi}^T\boldsymbol{D}^T\boldsymbol{\lambda} = 0 \end{cases} \tag{37}$$

the optimal games are

$$\begin{cases} \boldsymbol{u}^c = \boldsymbol{C}_1^{-1}\boldsymbol{B}^T\boldsymbol{\Phi}^T\boldsymbol{D}^T\boldsymbol{QDx}\left(t_f\right) \\ \boldsymbol{a}^p = -\boldsymbol{C}_2^{-1}\boldsymbol{C}^T\boldsymbol{\Phi}^T\boldsymbol{D}^T\boldsymbol{QDx}\left(t_f\right) \end{cases} \tag{38}$$

From Eq. (38), the optimal games are determined by the final state $\boldsymbol{x}(t_f)$, while the different games about pursuer and evader lead to different final state.

4.1 Evasion game in pursuer using DGL

Substituting the optimal games (Eq.(38)) into Eq.(26):

$$\dot{\boldsymbol{x}} = \boldsymbol{Ax} + \boldsymbol{BC}_1^{-1}\boldsymbol{B}^T\boldsymbol{\Phi}^T\boldsymbol{D}^T\boldsymbol{QDx}\left(t_f\right) - \boldsymbol{CC}_2^{-1}\boldsymbol{C}^T\boldsymbol{\Phi}^T\boldsymbol{D}^T\boldsymbol{QDx}\left(t_f\right) \tag{39}$$

Hence, the optimal games become:

$$\begin{cases} \boldsymbol{u}^c = \boldsymbol{C}_1^{-1}\boldsymbol{B}^T\boldsymbol{\Phi}^T\boldsymbol{D}^T\boldsymbol{QDP}^{-1}\boldsymbol{\Phi x}\left(t\right) \\ \boldsymbol{a}_{\mathrm{P}} = -\boldsymbol{C}_2^{-1}\boldsymbol{C}^T\boldsymbol{\Phi}^T\boldsymbol{D}^T\boldsymbol{QDP}^{-1}\boldsymbol{\Phi x}\left(t\right) \end{cases} \tag{40}$$

$$\boldsymbol{P} = \boldsymbol{I}_6 + \left(\int_0^{t_g} \boldsymbol{\Phi BC}_1^{-1}\boldsymbol{B}^T\boldsymbol{\Phi}^T dt_g\right)\boldsymbol{D}^T\boldsymbol{QD} - \left(\int_0^{t_g} \boldsymbol{\Phi CC}_2^{-1}\boldsymbol{C}^T\boldsymbol{\Phi}^T dt_g\right)\boldsymbol{D}^T\boldsymbol{QD} \tag{41}$$

where $\boldsymbol{I}_6$ is a 6×6 identity matrix, $\boldsymbol{u}^c$ is evasion DGL in pursuer using DGL (DGL/D).

4.2 Evasion game in pursuer using any other pursuit guidance law

In fact, evader cannot understand pursuit guidance law, so consider it to be a constant value and substitute the first equation of Eq. (38) into Eq. (26):

$$\dot{\boldsymbol{x}} = \boldsymbol{Ax} + \boldsymbol{BC}_1^{-1}\boldsymbol{B}^T\boldsymbol{\Phi}^T\boldsymbol{D}^T\boldsymbol{QDx}\left(t_f\right) + \boldsymbol{Ca}_{\mathrm{P}} \tag{42}$$

Hence, evasion DGL in pursuer using any other guidance law (DGL/A) is

$$\boldsymbol{u}^c = \boldsymbol{C}_1^{-1}\boldsymbol{B}^T\boldsymbol{\Phi}^T\boldsymbol{D}^T\boldsymbol{QDP}_1^{-1}\left(\boldsymbol{\Phi x} - \left(\int_0^{t_g}\boldsymbol{\Phi} dt_g\right)\boldsymbol{Ca}_{\mathrm{P}}\right) \tag{43}$$

$$\boldsymbol{P}_1 = \boldsymbol{I}_6 + \left(\int_0^{t_g} \boldsymbol{\Phi BC}_1^{-1}\boldsymbol{B}^T\boldsymbol{\Phi}^T dt_g\right)\boldsymbol{D}^T\boldsymbol{QD} \tag{44}$$

DGL/A is mature to the battlefield situation information, furthermore considering pursuit guidance law to be a constant value, so that DGL/A does not need to know the pursuer's game and need the pursuer acceleration from PMGKF only. This makes DGL excellent to other one-sided optimal evasion game.
$\boldsymbol{a}_{\mathrm{P}}$ in Eq. (43) can be calculated from Eq. (25):

$$\boldsymbol{a}_{\mathrm{P}} = \dot{\boldsymbol{v}}^p\tau_{\mathrm{P}} + \boldsymbol{v}^p \tag{45}$$

where $\dot{\boldsymbol{v}}^p$ can be estimated by difference about continued two filter results , but the result swings seriously. For decreasing this swing, difference filters results every 0.5s is substituted into Eq. (45). The equalized result error of pursuit acceleration is shown in Figure 6, and Figure 7 shows fractional error of approach velocity and relative distance by equalized result of pursuit acceleration.
Compare and contrast Figure 6 with Figure 4, estimated error decreases obviously after equalize the result error. But in less than two seconds after the beginning of game and in less than two seconds before the finish of confrontation, the equalized error is higher. Figure 7 shows the fractional error of approach and relative velocity is enough small to import of DGL coefficient matrix.

DOI: 10.13009/EUCASS2019-94

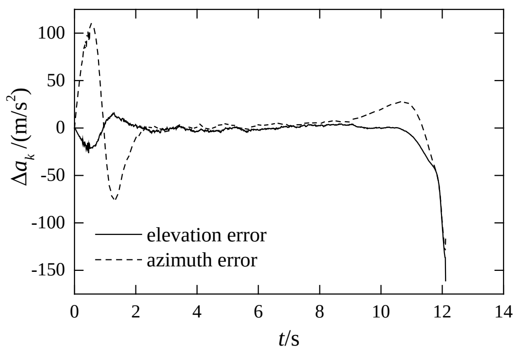

Figure 6 Equalized result error of acceleration

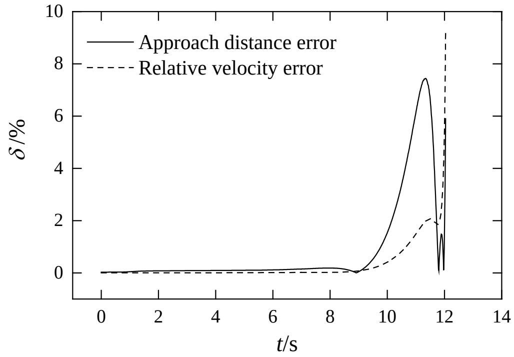

Figure 7 Fractional error of approach distance and relative velocity

4.3 Evasion game with the time delay of battlefield situation information

When the equalized error is enough little, evasion game is DGL/A by making the most of the equalized acceleration. When the equalized error is large, DGL/D is used to evader. In fact, the evader cannot understand the acceleration error, so that a differential game with adaptive weighted with the estimated error is impossible. Based on error laws on time estimated by simulation result, choosing different games is one of possible ways. In this paper, the acceleration error is enough small when t>2s and t_g<2s, evasion game is DGL/A, and other time DGL/D is used to evasion. That composes the differential game based on time list (DGL/T).

5. Numerical Simulation

Simulation import condition is the same as chapter 3.2, the parameter initialization is as Table 1. The evader can only aware the bearing-only information about pursuer and the other battlefield situation are all estimated by PMGKF. Simulation results are presented in Figures 8~13. Figures 8~10 show the evader actual accelerations under the three DGL. And pursuer games are estimated by PMGKF in Figures 11~13. The final miss distances under the three DGL and sine guidance law are shown in Table 2.

Initial elevation zero effort miss is little in Figure 2 while azimuth is large in Figure 3, which means initial elevation pursuit overload is larger than azimuth. Then evader takes the maximum azimuth acceleration (Figures 8~10), so that the zero effort miss is zoomed in to ensure successful evasion. But evasion game approaching the end of antagonism is not optimum under DGL/A because of the larger equalized error in t_g<2s (Figure 12). In elevation direction, evader all adopts changing maneuver acceleration value frequently game (Figures 8~10) for using the first order response dynamics of pursuer to evasion under the three DGL. The evader acceleration capability is so much lower than pursuer that the same game as azimuth direction is not effective under little initial zero effort miss.

Equalized result error time lists of pursuit acceleration under the three DGL are the same as that under sine law (Figure 6), namely the acceleration error is enough small when t>2s and t_g>2s in Figures 11~13. Then DGL/T based on time list is predicated correctly, and it is one of effective evasion games under bearing-only information in reality pursuit-evasion condition.

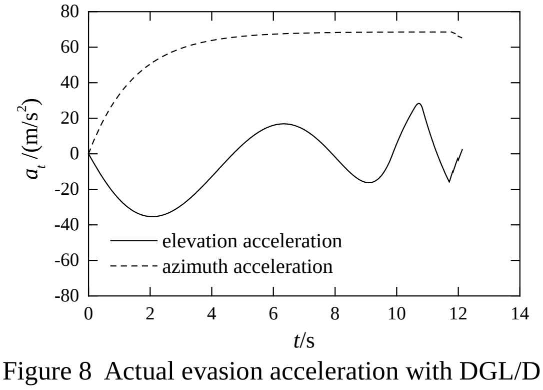

Figure 8 Actual evasion acceleration with DGL/D

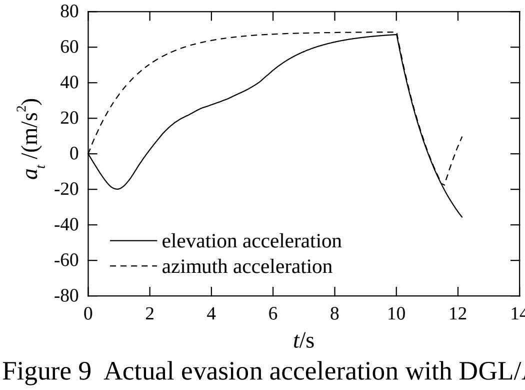

Figure 9 Actual evasion acceleration with DGL/A

DOI: 10.13009/EUCASS2019-94

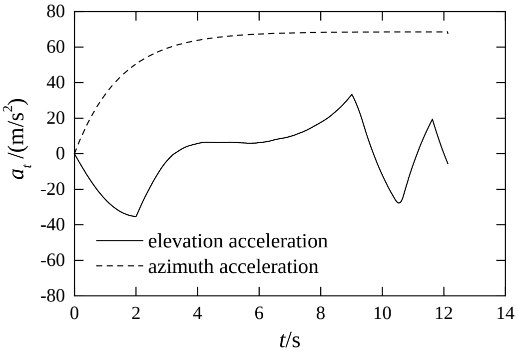

Figure 10 Actual evasion acceleration with DGL/T

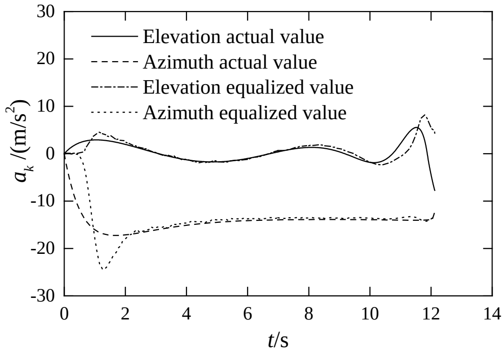

Figure 11 Equalized result of pursuit acceleration with DGL/D

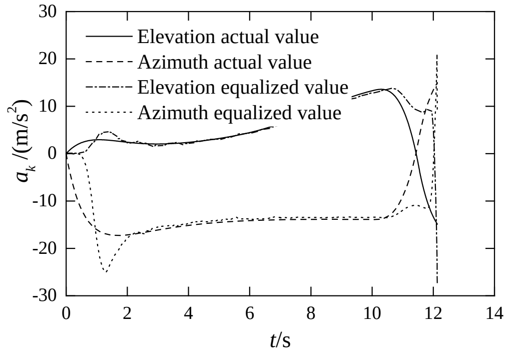

Figure 12 Equalized result of pursuit acceleration with DGL/A

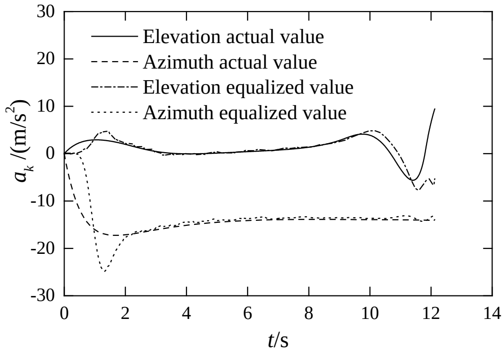

Figure 13 Equalized result of pursuit acceleration with DGL/T

Table 2 Comparison result of final miss distance

Guidance law	Miss distance/m
DGL/T	14.2639
DGL/D	9.4870
DGL/A	9.1377
Sine	2.8401

In normal circumstances, the maximum warhead lethal radius of air-to-air missile is 9 m. Then compared with the results of the final miss distance in Table 2, evader with sine guidance law ends up with unacceptable little miss distance, while using three DGL succeed in escaping pursuer. For further compared and contrasted evasion performance with three DGL, sine guidance law was tested with 1000 Monte Carlo simulation with different initial rate of LOS. The 813 final successful evasion situations is chosen to tested on three different DGL, statistical result of final evasion is shown in Figure 14.

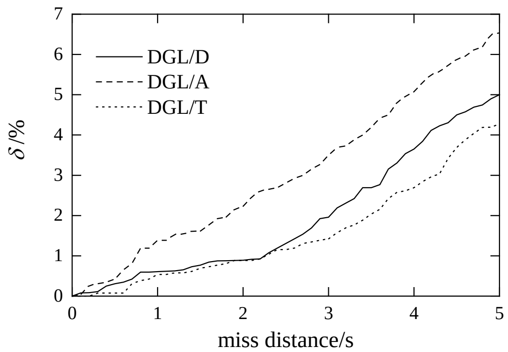

Figure 14 Statistical result of miss distance

Figure 14 shows that the probability of all three DGL is beyond 90%. DGL/A utilized the equalized information directly is the same as using the false information because of the larger equalized error in t<2s and t_g<2s. So the evasion result is the worst in three DGL. Pursuit game considered to DGL, DGL/D is a conservative game and a

DOI: 10.13009/EUCASS2019-94

hypo-optimal game in differential game. So that evasion result is better than DGL/A, but is not the optimal game all the same. The off-line simulation results are fully used in DGL/T, in this game, the different games are chosen with different equalized errors, so that the evasion result is the best in three different DGL. But the proportion of evasion cannot be 100% with any one of three DGL because the most overload and maneuver performance of evader are all lower than pursuer. Therefore, with the zero initial error, the other more effective game is needed to consider.
The superior evasion performance and practicability in engineering is improved within utilizing the bearing-only situation awareness adequately of DGL/T.

6. Conclusion

1) A pseudo-measurement gain Kalman filter is built in bearing-only information application, and a new differential game is designed based on the equalized error of pursuer's acceleration.
2) This filter can aware the entire situation between pursuer and evader, and this DGL can fully use the time law of equalized error of pursuer's acceleration to improve the evasion performance. The effectiveness is verified by simulation.
3) This DGL provides a self-contained real time maneuver game for evader. The evader's survivability can be increased by the DGL.

References

[1] Isaacs, R., Differential Games, Wiley, New York, 1965, pp. 278-280.
[2] Mauro, P., and Bruce, A. C., "Optimal interception of evasive missile warheads: numerical solution of the differential game," Journal of Guidance, Control, and Dynamics, Vol. 31, No. 4, 2008, pp. 1111-1122.
[3] Zarchan, P., Tactical and Strategic Missile Guidance, Vol. 176, Progress in Astronautics and Aeronautics, AIAA, Washington D. C., 1997.
[4] Shinar, J. and Steinberg, D., "Analysis of optimal evasive maneuvers based on a linearized Two-dimensional kinematic model," Journal of Aircraft, Vol. 14, No. 8, 1977, pp. 795-802.
[5] Ben-Asher, J., Cliff, E. M., and Kelley, H. J., "Optimal evasion with a path-angle constraint and against two pursuers," Journal of Guidance, Control, and Dynamics, Vol. 11, No. 4, 1988, pp. 300-304.
[6] Forte, I., Steinberg, A., and Shinar, J., "The effects of non-linear kinematics in optimal evasion," Optimal Control Application and Methods, Vol. 4, 1983, pp. 139-152.
[7] Shima, T, Shinar, J, and Weiss, H., "New interceptor guidance law integrating time varying and estimation delay models," Journal of Guidance, Control and Dynamics. Vol. 26, No. 2, 2003, pp. 295-303.
[8] Chen, R. H., Speyer, J. L., and Lianos, D., "Optimal intercept missile guidance strategies with autopilot lag," Journal of Guidance, Control, and Dynamics, Vol. 33, No. 4, 2010, pp. 1264-1272.
[9] Bardhan, R., and Ghose, D., "Nonlinear differential games-based impact-angle-constrained guidance law," Journal of Guidance, Control, and Dynamics, Vol. 38, No. 3, 2015, pp. 384-402.
[10] Zhang, P., Fang, Y. Zhang, F., Xiao, B., Hu, S., and Zong, S., "An adaptive weighted differential game guidance law," Chinese Journal of Aeronautics, Vol. 25, No. 5, 2012, pp. 739-746.
[11] Shima, T., "Optimal cooperative pursuit and evasion strategies against a homing missile," Journal of Guidance, Control, and Dynamics, Vol. 34, No. 2, 2011, pp. 414-425.
[12] Garcia, E., Casbeer, D. W., and Pachter, M., "Cooperative strategies for optimal aircraft defense from an attacking missile," Guidance, Control, and Dynamics, Vol. 38, No. 8, 2015, pp. 1510-1520.
[13] Aidala, V. J. "Kalman Filter Behavior in Bearings-only Tracking Applications," IEEE Transactions on Aerospace and Electronic Systems, 1979; AES-15(1).